27th EPS Conference on Contr. Fusion and Plasma Phys. Budapest, 12-16 June 2000 ECA Vol. **24B** (2000) 944 -947

Dependence of Electron Thermal Transport on ν_e^*

G.M.D. Hogeweij, N.J. Lopes Cardozo, M.R. de Baar and the RTP team

FOM Instituut voor Plasmafysica 'Rijnhuizen', Associatie EURATOM-FOM, partner of the Trilateral Euregio Cluster, P.O.Box 1207, 3430 BE Nieuwegein, The Netherlands

1. Introduction

A way to estimate the performance of future large tokamaks like ITER, is the use of empirical scaling laws [1, 2]. However, the engineering parameters used in such scalings, do not provide insight in het physical mechanisms causing the observed scaling. Expressions based on dimensionless physical parameters could provide such insight, and thus more confidence in the upgrading of current tokamak devices to larger machines. For the electron thermal diffusivity (χ_e) such expression takes the following form [3, 4]:

$$\chi_e = \frac{T_e}{B} F(\rho_e^*, \beta, \nu_e^*, q, \epsilon, ...) \tag{1}$$

where T_e, B denote the electron temperature and magnetic field, ρ_e^* is the normalized Larmor radius, β the kinetic pressure divided by the magnetic pressure, ν_e^* the electron collisionality, q the safety factor, and ϵ the inverse aspect ratio. A similar expression can be written for χ_i. This paper deals with χ_e only, and the subscript e is dropped.

The way to determine the dependency of F on a particular parameter is to perform dimensionally similar discharges, in which this one parameter is varied as much as possible between discharges, whereas all other parameters are kept fixed. The four main dimensionless parameters scale in the following way with T, n, B, plasma current I_p and major, minor radius R, a:

$$\begin{aligned} \rho^* \sim T^{1/2} B^{-1} a^{-1} \quad &; \quad \beta \sim nTB^{-2} \\ \nu^* \sim nT^{-2} B I_p^{-1} R^{3/2} a^{1/2} \quad &; \quad q \sim B I_p^{-1} R^{-1} a^2 \end{aligned} \tag{2}$$

In a given machine, in principle any combination of values of these 4 parameters can be attained by suitable choice of the 4 engineering parameters I_p, B, n and input power P (the latter is to be chosen such that the desired value of T is achieved). Hence, by choosing suitable combinations of the set (I_p, B, n, P) a scan of one of the dimensionless parameters can be performed, keeping the other 3 dimensionless parameters fixed. In this paper, scans of ν^* in RTP are described.

The leading parameter in F is ρ^*; the next important parameters are ν^* and β. Transport models and empirical scalings predict: $F \sim (\rho^*)^\alpha$ with $\alpha = 1, 0, -1/2, -1$ (gyro-Bohm, Bohm, Goldston-like empirical scaling, stochastic, respectively). It has been reported from DIII-D and ATF that χ_e scales gyro-Bohm, whereas χ_i scales Goldston-like [5, 6]. Dimensionally similar discharges in DIII-D, TFTR and JET were successfully simulated with a combination of gyro-Bohm models [7]. Reports on particle transport are unequivocal [8, 9]. The dependence of ν^* and β was studied in, e.g. TFTR and JET [10, 11].

2. Experimental design of ν^* scans in RTP

The RTP tokamak ($R_0/a = 0.72/0.164$ m, $B \leq 2.4$ T, $I_p \leq 150$ kA, pulse duration ≤ 600 ms) is equipped with a comprehensive set of diagnostics with high spatial and temporal resolution. Crucial for the experiments reported here is the double pulse Thomson Scattering (TS) system, which measures T_e and n_e along a vertical chord through the centre of the plasma at 100 radial positions simultaneously, with a spatial resolution of 2.6 mm [12, 13]. ECH (110 GHz, $P_{ECH} \leq 350$ kW) is available for additional heating.

The dependence of the ECH power deposition radius (ρ_{dep}) on B limits the possible variation of B: in order to have comparable conditions, the ECH power must always be deposited close to the plasma centre. However, it was found in RTP that the shape of the T_e and n_e profile is independent of ρ_{dep} as long as $\rho_{dep} \leq \rho(q = 1)$ [14, 15], which is at 25-30% of a for $q_a = 5$ discharges. This allows to devise two dimensionally similar discharges, I (II), with heating on the HFS (LFS), each with $\rho_{dep} \simeq 0.25$, which corresponds to $\delta B \simeq 10\%$ and thus, see Eq.2, $\delta\nu^* \simeq 40\%$.

Alternatively, one can keep B fixed at the expense of leaving one of the other dimensionless parameters free, and *assume* a given dependence of F on this parameter instead. In view of the results mentioned in the Introduction, we have devised discharges with fixed β and q, and where ρ^* was kept free; in the analysis it was assumed that $F \sim \rho^{*1}$ (gyro-Bohm). Eq.2 then shows that a modest variation $\delta\rho^*$ in ρ^* corresponds to $\delta T = -\delta n = 2\delta\rho^*$ and a large variation $\delta\nu^* = -6\delta\rho^*$ in ν^*.

Both strategies have been pursued in RTP at different plasma parameters.

3. Experimental Results and Analysis

ECH was used for heating. The TS T_e and n_e profiles were taken at least 100 ms after switch-on of ECH, i.e. when full equilibrium had been reached. For better statistics, the two TS pulses (typically 0.5 ms apart) were averaged. The q profile was calculated from the measured TS profiles, taking neo-classical correction and bootstrap current into account. No T_i measurements were available; an educated guess for T_i was used instead. Due to the weak e-i coupling in RTP, $T_i \ll T_e$ in EC heated discharges, so the contribution of the ions to β is small and an error in T_i has only a weak effect on β.
It is known that the χ profile shows strong local variations, i.e. barriers and regions of high χ [14, 15]. In the present study we are only interested in the global behaviour of χ; therefore the input profiles for the evaluation of χ were strongly smoothed.

3.1. Experiments with fixed ρ^*

Fig.1 shows profiles of 2 discharges I and II where it was tried to keep ρ^*, β and q fixed, one with HFS and one with LFS ECH, both with ρ_{dep} just inside the $q = 1$ surface.
To assess the dependence of F on ν^*, we put $F \sim \nu^{*\zeta}$. In Fig.2 the ratios χ_I/χ_{II}, ${\nu^*}_I/{\nu^*}_{II}$ and F_I/F_{II} are plotted; we omit here the centre and edge of the plasma where it is difficult to determine χ. In the right panel also $({\nu^*}_I/{\nu^*}_{II})^\zeta$ is shown for $\zeta = -0.3$, -0.5 and -0.7. It turns out that $\zeta = -0.5 \pm 0.2$ is a good estimate in this case for the average in the region around mid-radius , $0.35 \leq \rho \leq 0.65$.
The same scenario was performed at lower I_p and lower n with similar result.

3.2. Experiments with fixed B

Fig.3 shows profiles of 3 discharges with the same B and as much as possible the same β and q. One sees that in this way a much larger variation of ν^* can be obtained, at the cost of a modest variation of ρ^*. As said before, we now need an assumption on the dependence of F on ρ^*. So we assume $F \sim \rho^* G$ (gyro-Bohm), and we put $G \sim \nu^{*\zeta}$. Fig.4 shows the ratios as in Fig.2 for the 2 extreme discharges of Fig.3, with G instead of F. Now the best fit is $\zeta = -0.3 \pm 0.1$ for the average in the region around mid-radius.
The same scenario was performed at higher I_p and n with similar result.

4. Discussion

The negative dependence of χ on ν^* is opposite to neo-classical dependence. Existing scaling laws exhibit a weak positive (negative) dependence for H-mode (L-mode) [1, 10]; the difference is presently not understood. Thus, the RTP-scaling matches well with existing L-mode scalings.

There appears to be a radial trend in the data: the absolute value of ζ tends to decrease with r. Whether this is a real feature, or an artefact of radial trends of other dimensionless parameters, cannot be decided on basis of the present data.

The present analysis neglects small-scale structures like transport barriers in χ, known to be present [14, 15]. Thus it might be that the ν^* dependence found is caused by a combination of different scalings of χ for barriers and inter-barrier regions.

Acknowledgements. This work was performed under the Euratom-FOM association agreement, with financial support from NWO and Euratom.

References

[1] Kaye, S.M., et al, *Nucl. Fusion* **37** (1997) 1303.
[2] ITER CONFINEMENT DATABASE AND MODELLING GROUP, in Plasma Physics and Controlled Nuclear Fusion Research 1994 (Proc. 15th Int. Conf. Sevilla, 1994), Vol.2, IAEA, Vienna (1995) 525.
[3] Cordey, J.G., et al, *Plasma Phys. Contr. Fusion* **38** (1996) A67.
[4] Mikkelsen, D.R. et al, *Phys. Plasmas* 4 (1997) 1362.
[5] Petty, C.C., et al, *Phys. Rev. Lett.* **74** (1995) 1763.
[6] Murakami, M., et al, Proc. 19th Conf. on Contr. Fusion and Plasma Phys., (1992) Vol. 1, p. 521-524.
[7] Kinsey, J.E., et al, *Phys. Plasmas* **3** (1996) 3344.
[8] Wade, M.R. et al, *Phys. Rev. Lett.* **79** (1997) 419.
[9] Baker, D.R. et al, *Nucl. Fusion* **40** (2000) 799.
[10] Christiansen, J.P. et al, *Nucl. Fusion* **NF 38** (1998) 1757.
[11] Petty, C.C., et al, *Nucl. Fusion* **38** (1998) 1183.
[12] Barth, C.J., et al, *Rev. Sci. Instrum.* **68** 3380 (1997).
[13] Beurskens, M.N.A., et al, *Plasma Phys. Contr. Fusion* **41**, 1321 (1999).
[14] Lopes Cardozo, *Plasma Phys. Contr. Fusion* **39** (1997) B303.
[15] Hogeweij, G.M.D. et al, *Nucl. Fusion* **38** (1998) 1881.

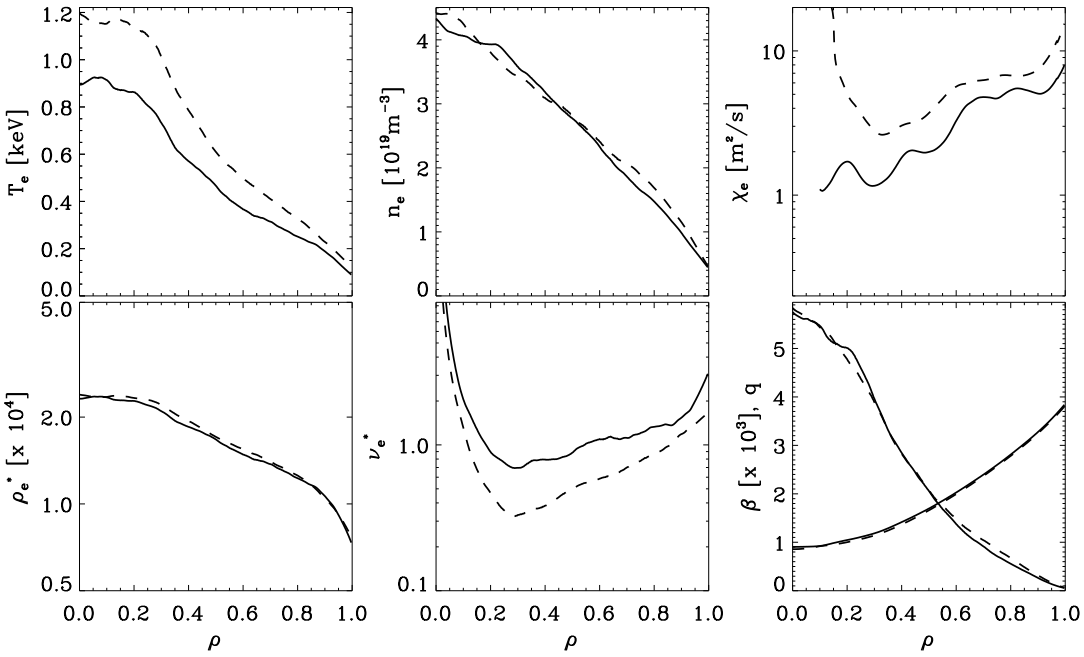

Figure 1: *Profiles of RTP discharges r19971119.073/068 (I/II, full/dashed lines). Plasma parameters:* $B = 1.88/2.10$ *T,* $I_p = 91/103$ *kA,* $P_{ECH} = 90/310$ *kW, respectively.*

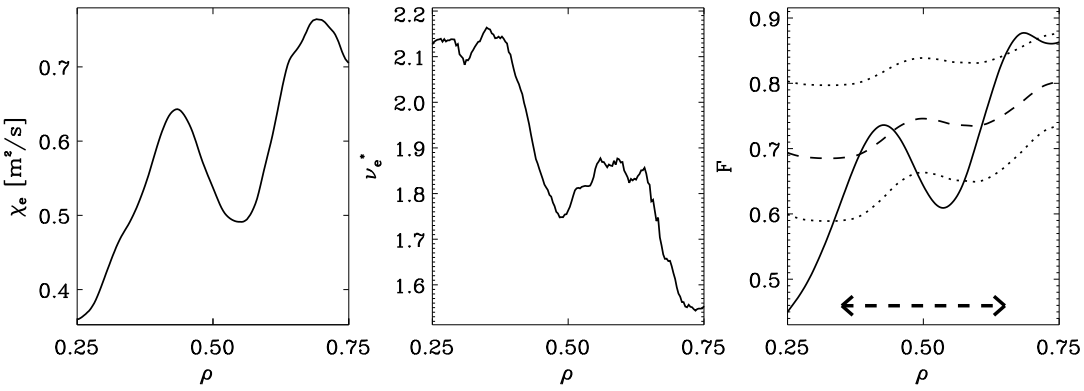

Figure 2: *Quotients χ_I/χ_{II}, $\nu^*{}_I/\nu^*{}_{II}$ and F_I/F_{II} for discharges I and II of Fig.1 (full lines). In the right panel also $(\nu^*{}_I/\nu^*{}_{II})^\zeta$ for $\zeta = -0.3, -0.5$ and -0.7 (dotted/dashed/dotted line).*

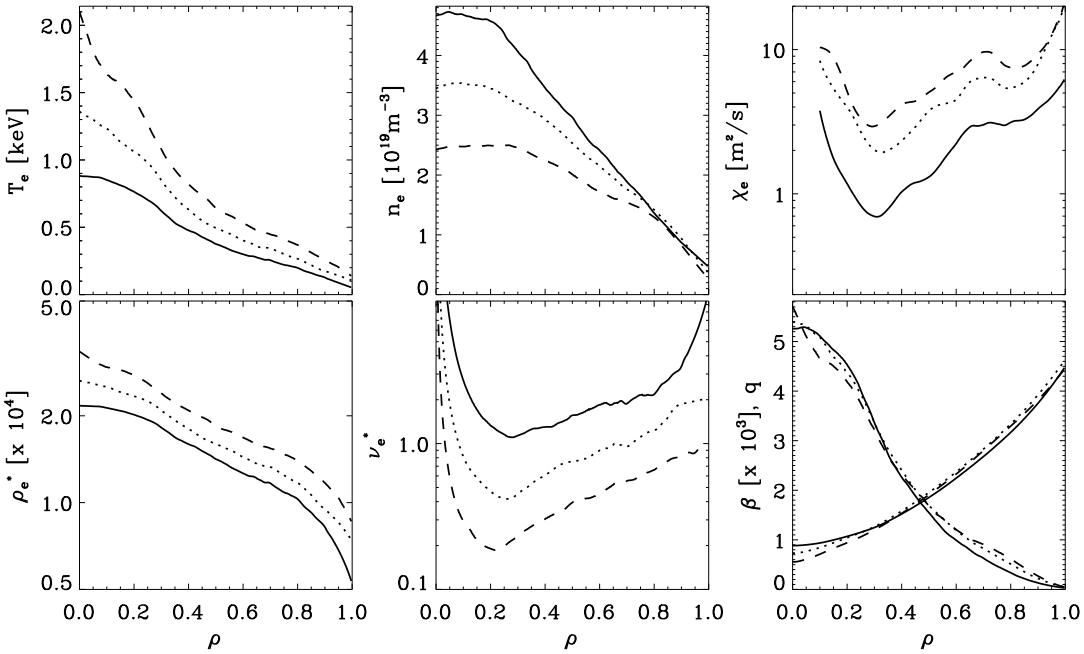

Figure 3: *Profiles of RTP discharges r19971119.062 (I,full), -058 (dotted), and -051 (II,dashed). Plasma parameters: $B = 2.00 - 2.02$ T, $I_p = 82$ kA, $P_{ECH} = 40, 200, 305$ kW, respectively.*

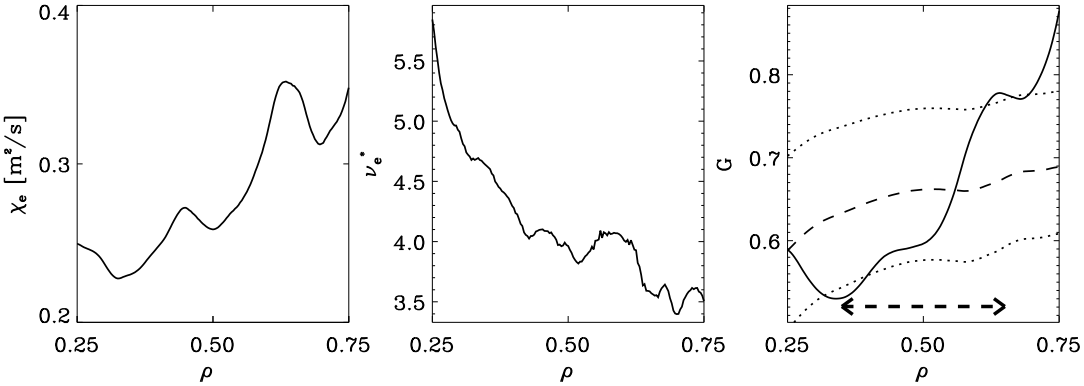

Figure 4: *Quotients as in Fig.2 for the discharges I and II of Fig.3 (full lines). In the right panel also $(\nu^*{}_I/\nu^*{}_{II})^\zeta$ for $\zeta = -0.2$, -0.3 and -0.4 (dotted/dashed/dotted line).*